JOURNAL OF MATERIALS SCIENCE 20 (1985) 1945–1952

Crack growth under static and cyclic loading in hot-stretched PMMA

M. KITAGAWA, H. KAJIWARA, H. KANZAKI
Department of Mechanical Engineering, Faculty of Technology, Kanazawa University, Kanazawa, Japan

T. ZHANG
Department of Mechanics, Beijing Chemical Engineering, Beijing, China

Crack growth behaviour under static and cyclic loading was investigated using anisotropic plates of PMMA oriented by hot-stretching. Both tests were performed at room temperature for samples with different degrees of orthotropy. A slight increase in the degree of orthotropy considerably improves the resistance to both static and cyclic crack growth in the case where the crack propagates perpendicularly to the hot-stretched direction. A power law relationship between crack growth rate and stress intensity factor may hold for both types of crack growth in the ranges of orthotropy tested. The experimental data for static crack growth were compared with a viscoelastic criterion based on the crack opening displacement theory for fracture. The criterion discussed here explains comparatively not only the beginning of cracking from a pre-introduced crack, but also the crack growth rate in oriented PMMA.

1. Introduction

Much effort has been made to understand the mechanism of static and fatigue crack growth in polymer solids generally recognized as isotropic. The results [1, 2] have demonstrated that fracture mechanics parameters such as stress intensity factor and strain energy release rate are useful for describing the crack growth rate in polymers as well as in metals. For the purpose of interpreting the relationship between the crack growth rate and the fracture mechanics parameters, fracture mechanics which takes into account the creep effect peculiar to polymer has been introduced by Williams [3] and the others [4–6]. According to their results, which give some predictions similar to each other, creep or relaxation processes play an important role in subcritical crack growth.

Practically used polymers are more or less anisotropic due to some forming processes. However, little attention has been paid to the experimental problems of a crack embedded in an orthotropic polymer, whereas there have been many published data on fibre-reinforced plastics (FRP) [7]. But the crack problem of FRP seems to be more complex than that of a simple polymer solid because of the mutual interaction between fibre and its matrix.

The purpose of this paper, therefore, is to investigate the relationship between crack growth rate and fracture mechanics parameters and to provide some interesting data using hot stretched PMMA plates under static and fatigue loading.

2. Experimental procedure

The material used was commercial poly(methyl methacrylate) (PMMA) plates 10 mm thick (Kyowa Gas Chemical Co, Japan). Rectangular sheets cut from them were uniaxially hot-streched at a slow tensile speed to the desired hot-stretching (HS) ratio λ, i.e. the ratio of the final to the initial length of the parallel part of the sheet, and were kept at that state for 30 min. This operation was performed at 125° C, slightly above the glass transition temperature in an electric oven. Then, they were slowly cooled down to room temperature. The stretched plates were not always uniform over the entire parts and were slightly thicker at their side edges than at the central part. The value

0022–2461/85 $03.00 + .12

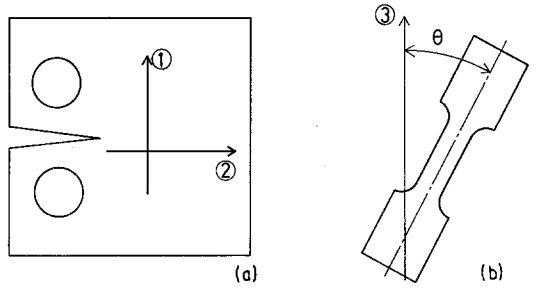

Figure 1 Schematic illustration of specimen orientation. (a) CT specimens 1 and 2 denote the HS directions for $\theta = 0°$ and 90° specimens, respectively. (b) Tensile specimen θ is the orientation angle.

of λ was determined as the ratio of the final to the initial values of the grid lines marked at the central part. The HS ratio λ was chosen in the ranges up to 3, otherwise the plates fractured viscoplastically. Besides these samples, as-received sheets, which were annealed for 1 h at 125° C, were also prepared to obtain the data for isotropic ($\lambda = 1$) crack behaviour.

Compact tension (CT) and dumb-bell-shaped specimens were machined from these plates so that the tensile axes were inclined at various angles to the HS direction. The schematic illustration of the specimen orientation is shown in Fig. 1. For the CT tests, the orientation angles $\theta = 0°$ and 90° mean that the crack growth directions are normal and parallel to the HS direction, respectively. The dimensions of the CT specimen are slightly different between specimens with different λ, but are geometrically similar to the standard geometry. The milled crack starter cut perpendicular to the tensile direction was pulled in an Instron-type testing machine to form an initial crack. In the case where λ is higher than 1.5 for a $\theta = 0°$ specimen, the crack does not always propagate along its initial axis. Then, a side groove 5 mm deep was cut along the initial crack axis to ensure straightforward crack growth. But the crack curved upwards or downwards even in the grooved specimen, and the experimental data were not obtained.

The static cracking experiments were performed by pulling the CT specimen at a constant crosshead speed ranging from 0.01 to 10 mm min^{-1}. The method for measuring the rates of crack growth were similar to the one used by Atkins, Lee and Caddell [8]. The crack growth rates were measured by a painted electrical resistance circuit in the path of the crack. The details of the experimental method have been reported elesewhere [8, 9].

The fatigue tests were carried out in the zero-tension load range. The maximum and the minimum loads were kept constant during the test. The loading frequency was in the ranges 0.4 to 0.6 Hz. The length of crack was measured by a travelling microscope. The growth rates were determined from the tangential slopes of a crack length against cycle diagram.

The stress intensity factor (SIF) K and its range ΔK were calculated from the equation

$$K \text{ or } \Delta K = F(P \text{ or } \Delta P)\sqrt{c}/WB \quad (1)$$

where P is the applied load, ΔP the range of applied load, c the crack length, W the width of specimen, B the thickness of specimen and F the correction factor described by

$$F = 29.6 - 185.5(c/W) + 655.7(c/W)^2 - 1017(c/W)3 + 638.9(c/W)^4.$$

The dumb-bell-shaped specimens with various values of λ and θ were pulled at a strain rate of about 5×10^{-5} sec^{-1} to measure static mechanical properties such as elastic modulus and fracture stress.

All the tests were performed at room temperature (25° C).

3. Viscoelastic fracture mechanics

We consider a crack in an infinite plate subjected to an applied stress σ at infinity. In a plane stress state, the stress σ_y and the crack opening displacement (COD) δ near the crack tip are given by

$$\sigma_y = K/\sqrt{2\pi r} \quad (2)$$

$$\delta = (8K/E)\sqrt{r/2\pi} = 8\epsilon\sqrt{\pi c}\sqrt{r/2\pi} \quad (3)$$

where $\epsilon (= \sigma/E)$ is the applied strain, c the half crack length, E the elastic modulus, and r the distance from the crack tip. When the plate is orthotropic, E should be replaced by

$$E = E_y[(2\sqrt{E_xE_y} + 4E_xE_y/E_{45} - E_x - E_y)/4E_x]^{-1/2} = \eta E_y \quad (4)$$

where the axis y is parallel to the loading direction and is coincident with one of the principal axes of orthotropy, E_x, E_y and E_{45} are the elastic moduli along the directions x, y and inclined at 45° to the x or y axis, respectively [10]. In the case where the material is isotropic, $\eta = 1$. As described later, in the ranges of the degree of orthotropy

tested here, η is nearly equal to unity. Then, for simplicity, η is set equal to unity and E_y, the modulus along the loading direction, is used in place of E.

Let us consider a linear viscoelastic crack growth criterion based on the above equations. At first, a condition under which the initial crack begins to grow and next, the growth rate of crack which continues to extend stably are discussed from the viewpoint of the COD theory for fracture.

The corresponding rule for a theory of viscoelasticity [11] may give

$$K = \int_0^t E(t-\tau)\frac{\partial}{\partial\tau}(\epsilon\sqrt{\pi c})\,d\tau \qquad (5)$$

where E is the relaxation modulus and t is the time. When the creep compliance D is approximated by Nutting's equation

$$D(t) = D_0 t^n$$

where D_0 and n are the material constants, $E(t)$ is described by

$$E(t) = E_0 t^{-n} \qquad E_0 = D_0^{-1}\sin(n\pi)/(n\pi) \qquad (6)$$

For a constant strain rate test, executing the integration of Equation 5 by use of Equation 6 leads to

$$K = \epsilon\sqrt{\pi c}(1-n)^{1+n}E_0(\dot{K}/K)^n \qquad (7)$$

where $\dot{K}$ is the rate of K with respect to t. If it is assumed that the crack begins to grow when δ at $r=\alpha$, α being a structural length, exceeds a critical level δ_c, Equations 3 and 7 give the critical stress intensity factor K_i for the beginning of crack propagation:

$$K_i = \frac{1}{1-n}\left[\frac{E_0\delta_c}{8}\sqrt{\frac{\alpha}{2\pi}}\right]^{1/(1+n)}\dot{K}^{n/(1+n)} \qquad (8)$$

Equation 8 shows that K_i increases with an increase in $\dot{K}$.

For a growing crack, the viscoelastic COD may be constructed from Equation 3 as follows [5]:

$$\delta = \delta_0 + \int_{t_x}^t D(t-\tau)\dot{\delta}_0(\tau)\,d\tau \qquad (9)$$

where δ_0 is the elastic counterpart of δ, t_x is the time at which the tip of a growing crack reaches the point x. When $t - t_x \ll t$, the first approximation of Equation 9 is written by [5]

$$\delta = \delta_0 D(\Delta t) \qquad (10)$$

where $\Delta t = t - t_x$. Assuming the COD criterion similarly to the case of a crack initiation, leads to

$$\dot{c} = \alpha\left[\frac{8D_0}{\delta_c}\sqrt{\frac{\alpha}{2\pi}}\right]^{1/n}K^{1/n} \qquad (11)$$

where Δt in Equation 10 is replaced by $\alpha/\dot{c}$, $\dot{c}$ being the crack growth rate.

As supposed from Equation 3, the constant $\delta_c/(8\sqrt{\alpha/2\pi})$ may denote a kind of a critical strain intensity factor. Then, we rewrite this constant as

$$M_c = \delta_c/(8\sqrt{\alpha/2\pi}) \qquad (12)$$

This concept, which has been called T-criterion by Kishimoto *et al.* [12], is successfully applied to isotropic crack behaviour. The governing Equations 8 and 11 derived from the COD theory for fracture may determine not only the beginning of crack extension, but also the crack propagation in a viscoelastic material. In the next section, these equations are compared with experimental results for both isotropic and orthotropic PMMA plates.

4. Results and discussion

4.1. Static mechanical properties

Fig. 2 shows the effect of λ on fracture stress σ_f, elastic modulus E and Poisson's ratio ν for both $\theta = 0°$ and $90°$. The rate of increase in σ_f with λ for $\theta = 0°$ is very small compared with the

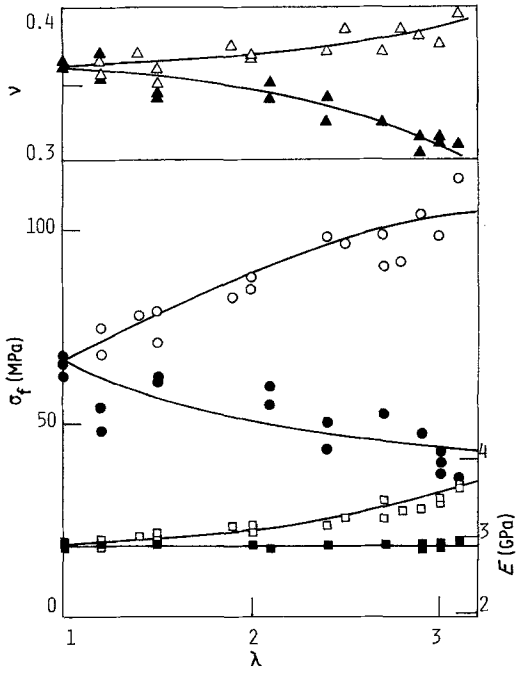

Figure 2 Dependence of fracture stress σ_f, elastic modulus E and Poisson's ratio ν on HS ratio λ.

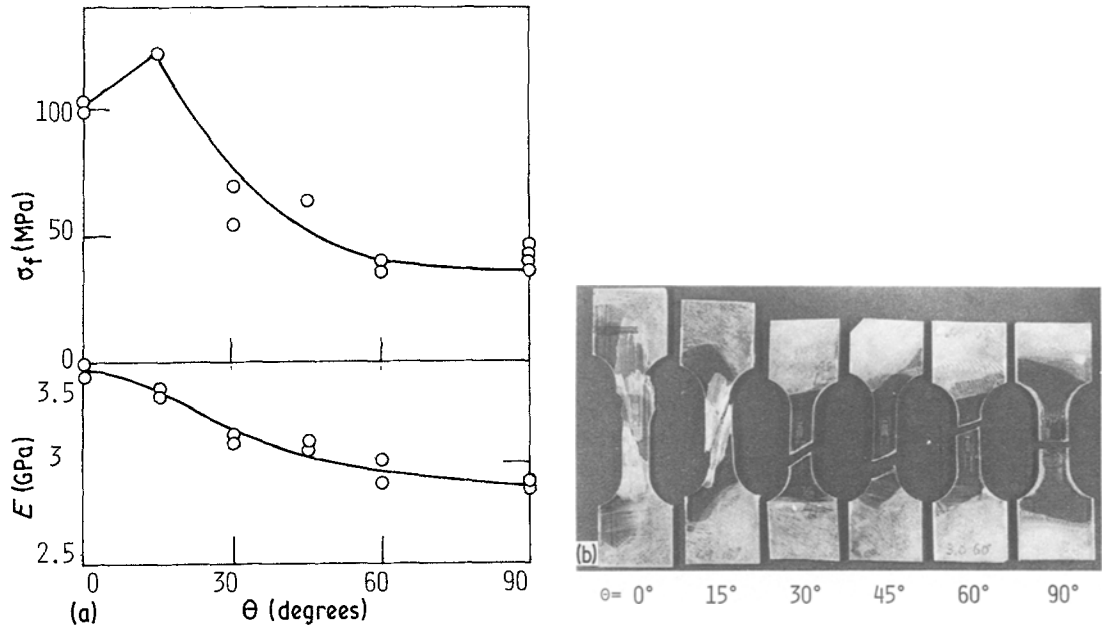

Figure 3 Effect of orientation angle θ on fracture stress σ_f and elastic modulus E (a) and fracture aspect (b).

published data of crystalline polymers such as PP [13]. For highly oriented PP with $\theta = 0°$, σ_f is known to become about 6 times higher than that for the isotropic specimen. But in PMMA used here, σ_f for $\lambda = 40$ was 1.7 times at most higher than σ_f for $\lambda = 1$.

The dependence of σ_f and E on the specimen orientation for $\lambda = 3$ is shown in Fig. 3, which also includes the fracture appearance. In the ranges from $\theta = 0$ to 30°, fracture initiates just after yielding probably due to a shear mode along the orientation direction and the fracture path becomes very irregular. As θ increases in excess of 30°, fracture occurs before yielding and its path becomes smooth. The angle between the tensile axis and the fracture plane tends to increase with increasing θ. When $\theta = 90°$, the path is perpendicular to the tensile axis.

From these results, the factor η mentioned in Section 3 can be calculated. For example, the computed values of η are 0.97 for $\lambda = 2$, $\theta = 0°$, 1.01 for $\lambda = 2$, $\theta = 90°$ and 1.04 for $\lambda = 3$, $\theta = 90°$. These values may be recognized as being close to unity. This may show that in the ranges of λ tested, the factor η is not so important for inferring the crack behaviour. In this paper, therefore, the value of η is set equal to unity.

The creep compliances D for both $\theta = 0°$ and 90° specimens with different λ were measured at temperatures of 0, 10 and 20° C in a home-made creep testing machine of a dead-weight type. An example of the variation of D with time t is shown on a log–log diagram in Fig. 4. The data at 0° and 10° C are shifted parallelly along the t-axis so that they may be superimposed on the result at 20° C. From the least square method of the shifted results, the constants D_0 and n were determined. To avoid the arbitrary shift, these calculations were carried out by a microcomputer. The calculated results are listed in Table I. It is shown that D_0 slightly depends on both λ and θ, but n is nearly insensitive to them. In this paper, therefore,

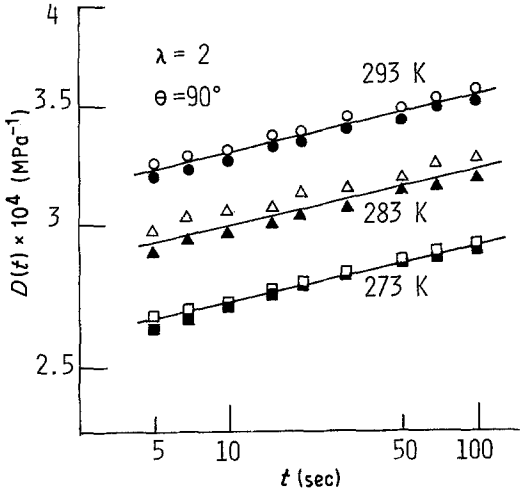

Figure 4 Variation of creep compliance D with time t at different temperatures.

TABLE I Creep constants and fracture parameters

λ	θ (degree)	$D_0 \times 10^4$ (in MPa sec)	$n \times 10^2$	$M_c \times 10^4$ ($m^{1/2}$)	COD $\times 10^6$ (m)
1		2.88	3.4	2.83	3.8
1.2	0	2.86	3.4	4.17	5.6
	90	2.91	3.4	3.00	4.0
1.5	0	2.88	3.4	4.85	6.5
	90	2.92	3.3	2.74	3.7
2	0	2.77	3.5	–	–
	90	2.96	3.3	2.62	3.5
2.7	0	2.70	3.5	–	–
	90	3.06	3.4	2.32	3.1

$n = 0.035$ is used for the calculation of Equations 8 and 11.

4.2. Crack growth under constant crosshead speed

In the CT test, the load P linearly increases with an increase in the applied displacement until it reaches a peak load P_m. Exceeding P_m, P gradually decreases owing to the continuous crack propagation. Some observations, which were made of the crack tip through a travelling microscope during the test, showed that the initial crack began to grow at a load P_i lower than P_m. The ratios P_m/P_i measured for isotropic samples were 1.15 to 1.25, which were nearly insensitive to the crosshead speed over the entire range tested. This indicates that the SIF K_m estimated from P_m does not correspond to the true value for crack initiation, K_i. Then, rewriting Equation 8 by use of $K_m = \xi K_i$, $\xi = P_m/P_i$ being the proportionality constant, one can obtain

$$K_m = \frac{\xi}{1-n} [E_0 M_c]^{1/(1+n)} \dot{K}^{n/(1+n)} \quad (13)$$

In Fig. 5, the values of K_m are plotted as a function of $\dot{K}$ for specimens with different degrees of orthotropy. It is found that (1) in the whole degrees of orthotropy tested, K_m slightly increases with increasing $\dot{K}$ as expected from Equation 13, and (2) a slight orientation of polymer chains due to hot stretching considerably improves the resistance to crack initiation for $\theta = 0°$, but does not so reduce it for $\theta = 90°$.

The solid lines in Fig. 5 are drawn based on Equation 13 with the values of E_0 and n mentioned in Subsection 4.1. The true initiation load P_i will be smaller than the experimentally measured value because of an infinitesimal crack growth unobserv-

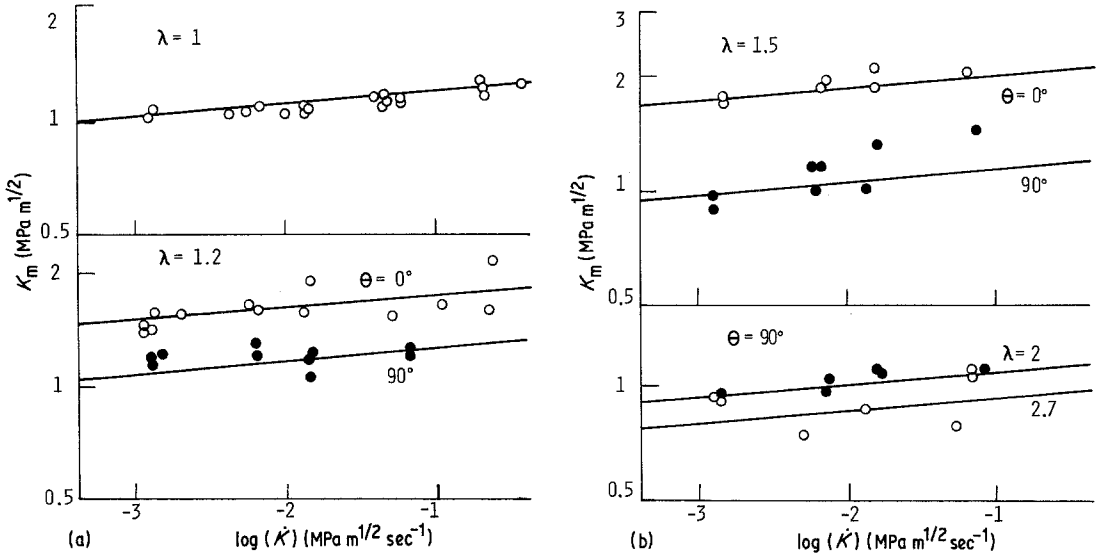

Figure 5 Critical stress intensity factor K_m for the initiation of crack growth as a function of the rate of stress intensity factor $\dot{K}$ at various values of λ and θ.

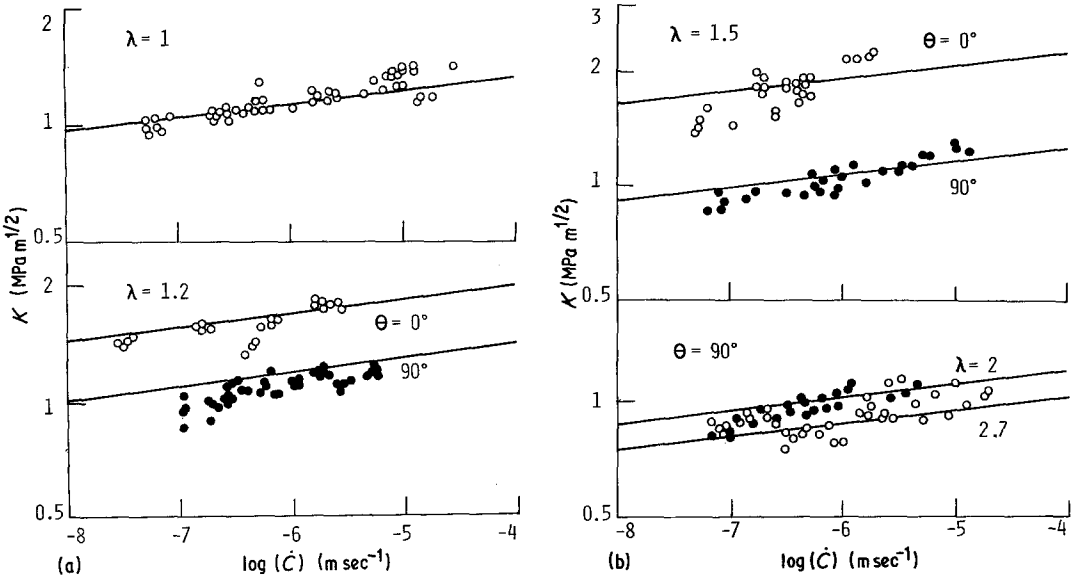

Figure 6 Stress intensity factor K as a function of crack growth rate $\dot{c}$ for various values of λ and θ. The solid lines are theoretical.

able through the microscopy, and then the ratio P_m/P_i is to be higher than 1.15 to 1.25. In this paper, therefore, $\xi = 1.3$ is used for the calculation and its value is assumed to be independent of $\dot{K}$ and λ. The values of M_c, which are determined so that the equation may fit the experimental data, are listed in Table I.

Fig. 6 shows the experimental relationships between crack growth rate $\dot{c}$ and K for various orthotropic samples. As expected from Equation 11, a power law relationship between $\dot{c}$ and K may hold for the entire ranges of $\dot{c}$ tested. A slight increase in λ greatly improves the resistance to crack growth as well as its initiation resistance for $\theta = 0°$. The solid lines in Fig. 6 denote Equation 11 with the same values of M_c as used for the theoretical calculation of K_m. The structural length α is set equal to the mean half craze length (1.75×10^{-5} m) measured over the range of $\dot{c}$ from 10^{-8} to 10^{2} mm sec^{-1} using isotropic samples by Döll [13]. The values of COD calculated from the above-mentioned values of M_c using $\alpha = 1.75 \times 10^{-5}$ m are listed in Table I. Practically, the structural length α may be influenced by the degree of orthotropy. But from the nature of Equation 11, a slight change in α does not so affect the place of the theoretical lines on a double logarithmic diagram. Then, for convenience sake, α is assumed to be independent of both λ and θ. The values listed in Table I are higher than the mean value observed by Döll (2.7×10^{-6} m). Table I shows that as λ increases, M_c steeply increases for $\theta = 0°$, but slightly decreases for $\theta = 90°$. In other words, M_c itself directly corresponds to the cracking resistance. Therefore, M_c is able to become an important material constant for estimating the viscoelastic cracking resistance.

A good agreement between the theoretical and the experimental results may indicate that the theory developed here is available for inferring not only the growth stage of crack, but also its initiation.

4.3. Fatigue crack growth

Except for $\theta = 0°$ specimens, fatigue crack generally grows along its initial axis with an increase in loading cycle. In the case of $\theta = 0°$ specimens with relatively high λ, however, it departs from its initial crack plane and curves upwards or downwards. The higher the HS ratio, the more distinctive this trend is. This aspect is clearly observed in Fig. 7. Then, the crack growth rates for $\theta = 0°$ were measured only at the early stage where the crack propagated almost along its initial axis. In the case where λ is higher than 1.5, the growth rates could not be measured because of the sharply curved crack growth.

Fig. 8 shows a ΔK against crack growth rate dc/dN diagram for different degrees of orthotropy. The solid lines are drawn empirically. A slight increase in λ improves the resistance to fatigue crack growth as well as creep crack growth for

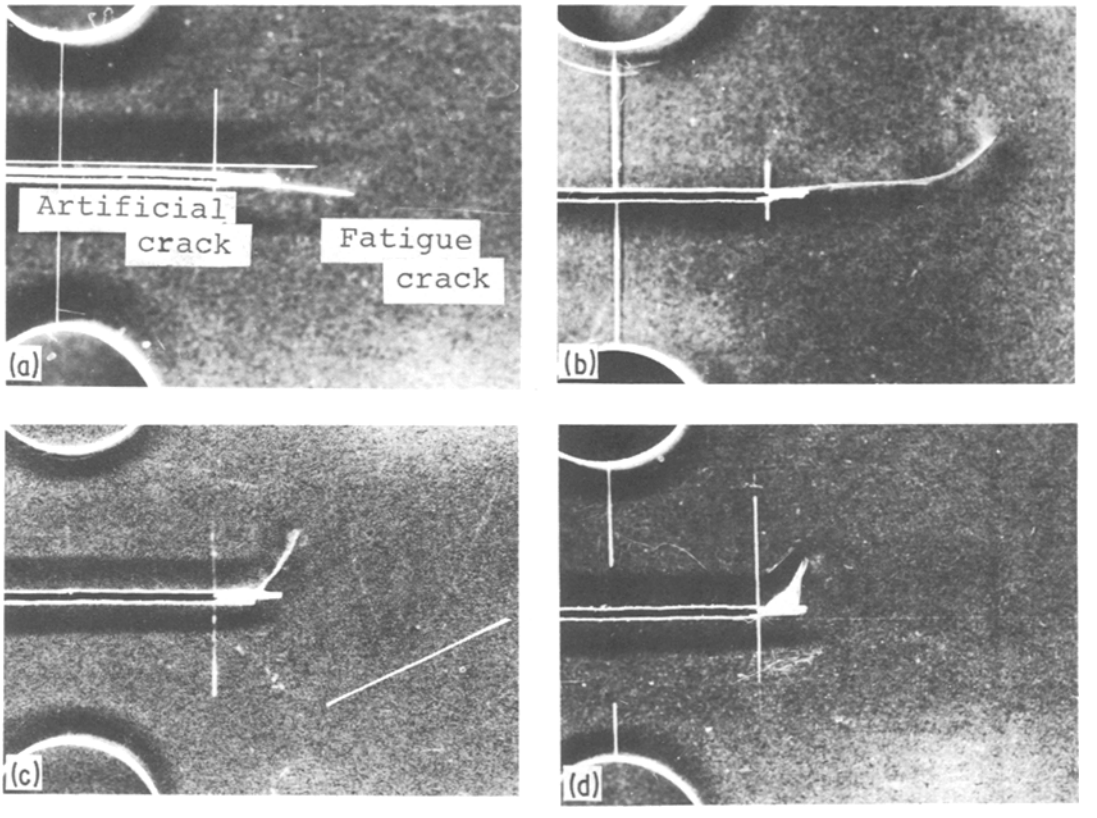

Figure 7 Fatigue crack growth directions for $\theta = 0°$ specimens with different values of λ. (a) $\lambda = 1$, (b) $\lambda = 1.5$, (c) $\lambda = 2$, (d) $\lambda = 2.7$.

$\theta = 0°$. The usually used power law

$$dc/dN = A(\Delta K)^m \qquad (14)$$

may be valid for the entire ranges of λ and θ tested. But as is evident from Fig. 8, there exist two regions, i.e. Region I at low values of ΔK and Region II at high values of ΔK. The slope m in each region seems to be independent of the degree of orthotropy, but is different between Region I and II. The value of $m = 30$ in Region II is nearly equal to that of creep crack growth. The fracture surface in Region II is smooth and is similar to

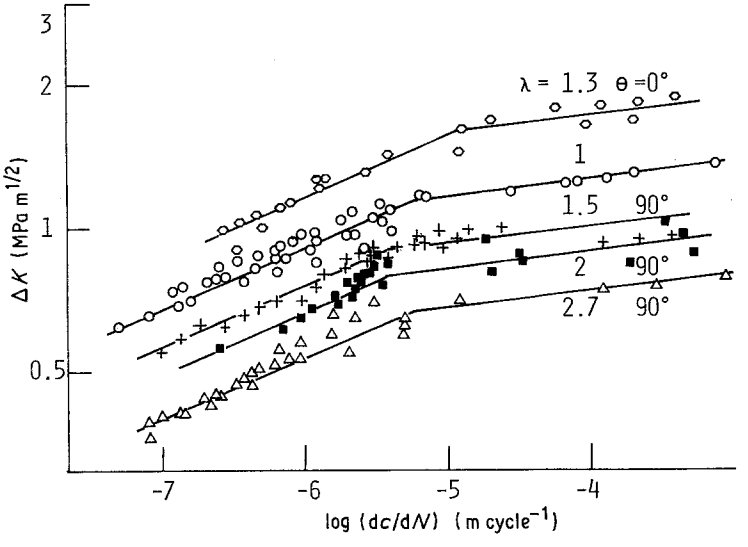

Figure 8 Stress intensity factor range ΔK as a function of fatigue crack growth rates dc/dN for different values of λ and θ. The solid lines are empirical.

that of creep crack growth. These may show that the crack growth in Region II is mainly governed by the creep damage as predicted in Subsection 4.2 and therefore, is able to be anticipated from Equation 11. Future work will be needed. On the other hand, the crack behaviour in Region I may be determined by cyclic damage which is difficult to evaluate quantitatively.

5. Conclusions

The crack growth of orthotropic PMMA under static and cyclic loading were investigated, and were discussed based on the COD criterion for fracture. The results are summarized as follows:

1. A slight increase in the degree of orthotropy greatly improves the resistance to both static and fatigue crack growth in the direction normal to the HS direction. This improvement may be attributed partly to the change of creep compliance and mainly to the increase in the critical COD.

2. The criterion derived from the COD theory explains well not only the beginning of crack growth, but also the crack propagation under static loading.

Acknowledgement

We are grateful to Mr H. Asano for his technical assistance.

References

1. G. P. MARSHALL and J. G. WILLIAMS, *Plast. Polym.* **38** (1970) 95.
2. R. W. HERTZBERG and J. A. MANSON, "Fatigue of Engineering Plastics" (Academic Press, New York, 1980).
3. J. G. WILLIAMS and G. P. MARSHALL, *Proc. Roy. Soc.* **A342** (1975) 55.
4. W. G. KNAUSS, *Int. J. Fract. Mech.* **6** (1970) 7.
5. M. P. WNUK, *ibid.* **7** (1971) 383.
6. R. A. SCHAPERY, *Int. J. Fract.* **11** (1975) 141.
7. J. TIROSH, *J. Appl. Mech., Trans. ASME* **40** (1973) 785.
8. A. G. ATKINS, C. S. LEE and R. M. CADDELL, *J. Mater. Sci.* **10** (1975) 1381.
9. M. KITAGAWA, *J. Soc. Mater. Sci. Jap.* (in Japanese) **29** (1980) 1142.
10. D. D. ANG and M. L. WILLIAMS, *J. Appl. Mech., Trans. ASME* **28** (1961) 372.
11. R. M. CHRISTENSEN, "Theory of Viscoelasticity" (Academic Press, New York, 1971).
12. K. KISHIMOTO, S. AOKI, Y. IZUMIHARA, N. SHIMIZU and M. SAKATA, *J. JSME* (in Japanese), **49** (1981) 347.
13. W. DÖLL, M. G. SCHINKER and L. KOENCZOEL, *Int. J. Fract.* **15** (1979) R145.

Received 2 April
and accepted 18 June 1984